POLITECNICO DI TORINO
Repository ISTITUZIONALE

Dynamic Modeling and Performance Assessment of a Mechanical Power Take-Off System for Ocean Wave Energy

Original
Dynamic Modeling and Performance Assessment of a Mechanical Power Take-Off System for Ocean Wave Energy / Mura, A., Mazza, L., Canavese, G., Margaria, L.. - In: ENGINEERING PROCEEDINGS. - ISSN 2673-4591. - ELETTRONICO. - 131:1(2026), pp. 1-12. [10.3390/engproc2026131043]

Availability:
This version is available at: 11583/3013030 since: 2026-07-13T12:49:03Z

Publisher:
MDPI

Published
DOI:10.3390/engproc2026131043

Terms of use:

This article is made available under terms and conditions as specified in the corresponding bibliographic description in the repository

Publisher copyright

(Article begins on next page)

08 October 2026

engineering proceedings

MDPI

Proceeding Paper

Dynamic Modeling and Performance Assessment of a Mechanical Power Take-Off System for Ocean Wave Energy †

Andrea Mura [1,*], Luigi Mazza [1], Giancarlo Canavese [2] and Luca Margaria [1]

[1] Department of Mechanical and Aerospace Engineering, Politecnico di Torino, 10129 Torino, Italy; luigi.mazza@polito.it (L.M.); luca.margaria@polito.it (L.M.)
[2] Department of Applied Science and Technology, Politecnico di Torino, 10129 Torino, Italy; giancarlo.canavese@polito.it
* Correspondence: andrea.mura@polito.it
† Presented at the 54th Conference of the Italian Scientific Society of Mechanical Engineering Design (AIAS 2025), Florence, Italy, 3–6 September 2025.

Abstract

Wave energy represents one of the most promising renewable sources due to its high energy density and predictable availability compared to wind and solar power. Despite its potential, technological exploitation remains challenging because of harsh marine environments, high installation and maintenance costs, and the absence of a dominant technology. This work presents a comprehensive review of wave energy conversion technologies and provides a detailed kinematic and dynamic analysis of a novel mechanical system designed to transform oscillatory linear motion into continuous unidirectional rotary motion, suitable for electricity generation. Particular focus is placed on the analytical modeling of the system, the design of a flywheel for energy stabilization, and performance evaluation. Results highlight the feasibility of the proposed configuration and its potential advantages compared to conventional hydraulic systems.

Keywords: wave energy conversion; renewable energy; mechanical system design; kinematic and dynamic analysis

1. Introduction

Renewable energy sources are central to the global energy transition, aiming to reduce carbon emissions and mitigate climate change. Among them, ocean wave energy has emerged as a highly promising resource due to its high energy density and relative predictability compared to solar and wind energy [1]. The potential contribution of wave power to the global electricity demand has been estimated at approximately 10%, representing a significant untapped resource.

Unlike wind and solar, whose availability is often intermittent and site-dependent, wave energy benefits from the continuous transfer of wind energy into the ocean surface, making its forecasting and integration into power grids more reliable [2]. However, despite decades of research and development, wave energy technology remains largely pre-commercial. Key barriers include the durability of materials in harsh marine environments, complex engineering requirements, high capital costs, and the lack of standardized and mature conversion systems [3].

Wave Energy Converters (WECs) encompass a wide variety of configurations and operating principles. To date, no single technology has emerged as dominant, with over one thousand patents registered worldwide [4]. This diversity reflects the experimental

Check for updates

Academic Editors: Nicola Bonora, Umberto Galietti, Luigi Bruno, Davide Castagnetti, Cristiana Del Prete, Mario Guagliano and Vigilio Fontanari

Published: 10 July 2026

Copyright: © 2026 by the authors. Licensee MDPI, Basel, Switzerland. This article is an open access article distributed under the terms and conditions of the Creative Commons Attribution (CC BY) license.

nature of the field and the difficulty of balancing energy capture, cost efficiency, reliability, and environmental integration.

This paper addresses two main objectives. First, it provides an overview of wave energy conversion technologies, including their classification by location, physical principle, and power take-off (PTO) system. Second, it develops a detailed kinematic and dynamic analysis of a proposed mechanical device that converts reciprocating motion into continuous rotary motion through rack-and-pinion and freewheel systems [5]. The system is completed with a flywheel dimensioning study to ensure smooth operation under the fluctuating input of ocean waves.

2. Wave Energy Conversion Technologies

2.1. Classification by Location

Wave energy conversion technologies can be classified based on their installation site [6]:

- Onshore: Devices integrated into coastal structures such as breakwaters or harbor walls. These benefit from easy accessibility and lower maintenance costs but operate with reduced wave energy intensity due to nearshore dissipation.
- Nearshore: Installed at moderate distances from the coastline (10–25 m depth). These systems balance energy capture with manageable installation and maintenance operations.
- Offshore: Located in deep waters, where wave energy is maximal. Offshore devices achieve higher efficiency but face higher installation, anchoring, and maintenance challenges [6].

2.2. Classification by Physical Principle

The working principle of the device defines its category [7]:

- Oscillating Water Columns (OWCs): Utilize air compression and decompression within a chamber to drive bidirectional turbines (Figure 1). They are technologically mature but limited by moderate efficiency (40–55%).

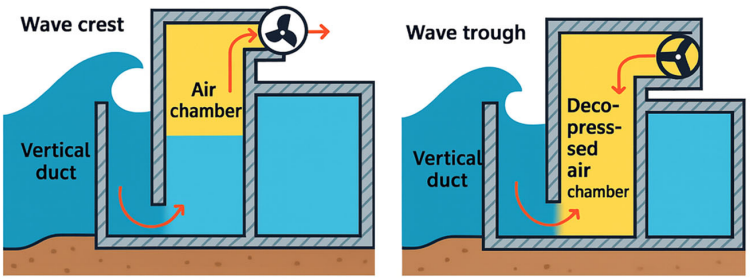

Figure 1. Oscillating Water Columns systems.

- Overtopping Systems: Capture wave crests in elevated reservoirs and release the stored water through hydraulic turbines (Figure 2). They provide relatively stable output but require massive infrastructure and achieve modest efficiency (15–25%).

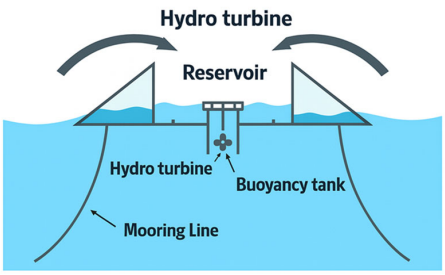

Figure 2. Overtopping systems.

- Oscillating Bodies: Exploit the motion of floating or submerged structures relative to a fixed reference (Figure 3). These include point absorbers, attenuators, and terminators, achieving potential efficiencies above 80% in controlled conditions. However, mechanical complexity and survivability in harsh seas are major issues [7].

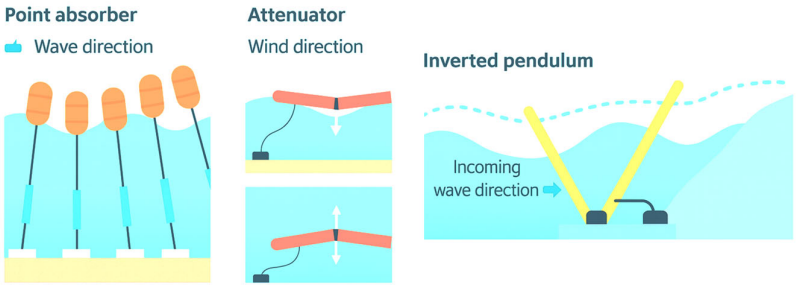

Figure 3. Oscillating body systems.

2.3. Classification by Power Take-Off (PTO) System

The PTO defines how mechanical energy is transformed into electricity [8–11]:

- Direct Mechanical Systems: Involve gears, levers, or linear generators to directly convert motion. They are simple and efficient (80–90%) but suffer from discontinuous input, requiring flywheels or other smoothing devices.
- Hydraulic Systems: Widely used in oscillating body devices, they employ pumps and high-pressure fluids driving hydraulic motors and generators. They allow energy regulation but suffer from friction losses and complexity.
- Pneumatic Systems: Typical of OWC devices, where airflow drives turbines. They are mechanically simple but limited by turbine efficiency (30–45%).

A summary comparison is reported in Table 1.

Table 1. Comparison of systems.

PTO Type	Efficiency	Complexity	Maintenance	Robustness	Cost
Mechanical	80–90%	Low–Medium	Medium	High	Low–Medium
Hydraulic	70–85%	High	Medium–High	Medium	High
Pneumatic	30–45%	Medium	Medium	Medium	Medium

2.4. Real-World Applications

Several pilot projects have demonstrated the feasibility of WECs:

- The LIMPET plant in Scotland is the first grid-connected commercial wave energy device, based on OWC technology [12].
- The OE-Buoy in Ireland, a floating OWC system reaching up to 2.5 MW [13].
- The Wave Dragon in Denmark, a floating overtopping device capable of 4 MW, combining wave and wind energy [14].
- The OBREC project in Italy, integrated into a breakwater at Naples harbor [15].
- Point absorbers such as Power Buoy and Archimedes Wave Swing [16].
- The ISWEC (Inertial Sea Wave Energy Converter) developed by Politecnico di Torino, using gyroscopic PTO [17].
- The Pelamis attenuator, tested in Portugal [18].
- Terminator-type devices such as Stingray, Oyster, and Eco Wave Power [19].

These case studies illustrate the richness of design solutions but also highlight difficulties in scaling prototypes into reliable commercial plants.

3. Description of the Proposed Mechanical System

The mechanical system investigated in this work is designed to transform an oscillatory linear motion, typical of ocean waves, into a continuous unidirectional rotary motion suitable for driving an alternator (Figure 4). The device integrates linear-to-rotary conversion, freewheel clutches, transmission elements, and an energy storage flywheel [5].

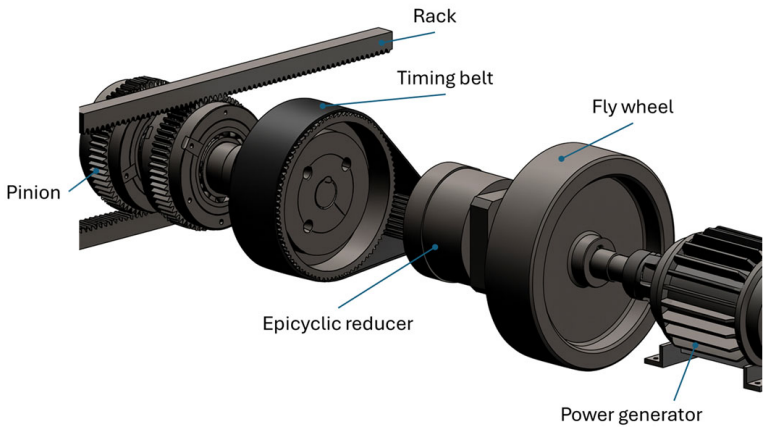

Figure 4. Mechanical system to transform oscillating linear motion into rotating unidirectional motion.

The system begins with two parallel racks, mounted within a rigid housing sliding horizontally along four ball-bearing guides. The housing is subjected to an external harmonic force of the type:

$$F(t) = F_0 \cdot sin\,(\Omega \cdot t) \quad (1)$$

where $F_0 = 5000$ [N] is the maximum applied force, and $\Omega = \frac{2\pi}{T}\left[\frac{\text{rad}}{\text{s}}\right]$ is the angular frequency corresponding to a wave period of t = 4 [s].

The racks mesh with two pinions, each equipped with a freewheel mechanism, and both pinions are coaxially mounted on a single shaft. The freewheels play a rectifying role: one engages when the housing moves in one direction, while the other engages when the motion reverses. This ensures that the output shaft always rotates in the same direction, effectively acting as a mechanical rectifier.

The primary shaft is then connected to a secondary shaft through a toothed belt transmission and an epicyclic gear train acting as a speed multiplier. The belt transmission ratio is 3.6, while the planetary gear provides an additional ratio of 10, giving a total multiplication factor of about 36. This arrangement elevates the output rotational speed to values suitable for an alternator.

To stabilize rotational speed and reduce oscillations induced by the reciprocating input, a flywheel is coupled to the secondary shaft. Its design is based on energy balance and degree of irregularity criteria, ensuring compatibility with alternator requirements [20,21].

4. Kinematic and Dynamic Analysis

The housing, and thus the racks, are subjected to the sinusoidal input force of Equation (1), Figure 5. Neglecting stiffness and damping effects in the first approximation, the displacement of the racks can be written as

$$x(t) = A \cdot sin(\Omega \cdot t) \quad (2)$$

with amplitude A = 0.5 m in the studied case.

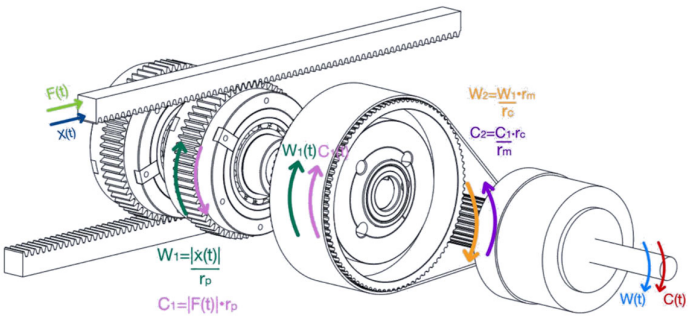

Figure 5. Free body diagram of the system.

Velocity:

$$a(t) = -A \cdot \Omega \cdot sin(\Omega \cdot t) \tag{3}$$

Acceleration:

$$a(t) = -A \cdot \Omega^2 \cdot sin(\Omega \cdot t) \tag{4}$$

The racks engage with pinions of primitive radius r_p = 90 mm. Thus, the angular velocity and angular acceleration of the first shaft are:

$$w_1(t) = \frac{|v(t)|}{r_p} = \frac{A}{r_p} \cdot \Omega \cdot |cos(\Omega \cdot t)| \tag{5}$$

$$\alpha_1(t) = \frac{dw_1}{dt} = -\frac{A}{r_p} \cdot \Omega^2 \cdot sin(\Omega \cdot t) \tag{6}$$

The corresponding torque transmitted to shaft 1 is

$$C_1(t) = |F(t)| \cdot r_p = F_0 \cdot r_p \cdot |sin(\Omega \cdot t)| \tag{7}$$

With a total gear ratio i = 36, the secondary shaft rotates at:

$$w_2(t) = w_1(t) \cdot i = \frac{A}{r_p} \cdot \Omega \cdot i \cdot |cos(\Omega \cdot t)| \tag{8}$$

$$\alpha_2(t) = \frac{dw_2}{dt} = -\frac{A}{r_p} \cdot \Omega^2 \cdot i \cdot sin(\Omega \cdot t) \tag{9}$$

while the torque becomes:

$$C_2(t) = \frac{C_1(t)}{i} = \frac{F_0 \cdot r_p}{i} \cdot |sin(\Omega \cdot t)| \tag{10}$$

The maximum mechanical power at the secondary shaft is therefore:

$$P_{m_{MAX}} = C_{2_{MAX}} \cdot w_{2_{MAX}} \tag{11}$$

The analysis reveals strong oscillations in angular velocity and torque due to the sinusoidal input force (Figure 6). Without additional stabilization, the alternator would operate under highly irregular conditions, leading to inefficiency and possible damage. This justifies the introduction of a flywheel, discussed in the following section, to regulate kinetic energy exchange and maintain acceptable rotational uniformity.

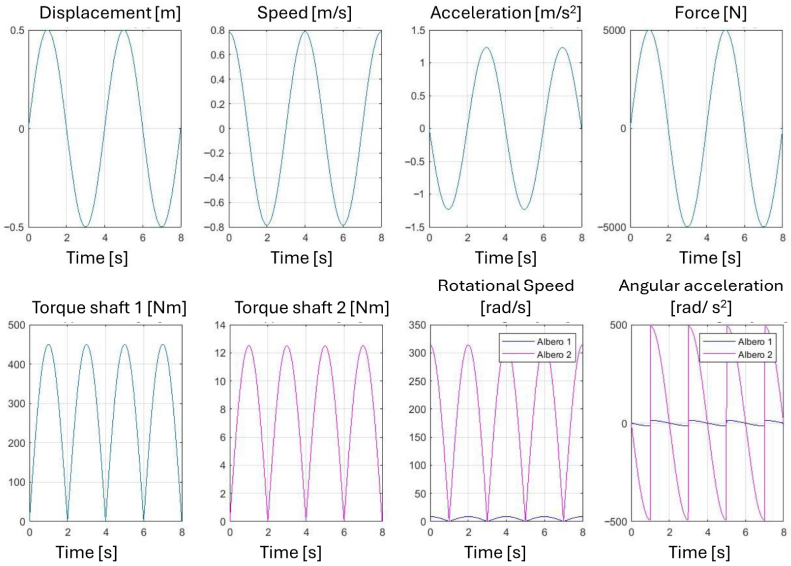

Figure 6. Kinematic and dynamic parameters vs. time.

Flywheel Design and Optimization

Alternators require a nearly constant rotational speed to operate efficiently. To quantify speed fluctuations, the degree of irregularity is defined as

$$i = \frac{w_{max} - w_{min}}{w_{mean}} \tag{12}$$

For typical alternators, i must be below 1/300 [20].

The system's inertia before including the flywheel is given by the sum of the inertias of the pulley, planetary gear, and coupling components:

$$J = J_{\mathrm{m}} + J_c + J_b + J_r \tag{13}$$

where J_{m}, J_c, J_b and J_r are the inertias of the motor pulley, driven pulley, conical bushing, and gear reducer, respectively.

The required total inertia to satisfy the degree of irregularity constraint is obtained from the energy balance equation for periodic systems:

$$i \cdot J_{TOT} \cdot w_{mean}^2 = \int_0^{\vartheta} (C_m - C_r)\, d\vartheta \tag{14}$$

where Cm is the driving torque, C_r the resistant torque, and θ the angular displacement.

Solving yields:

$$J_{TOT} = \frac{\int_{t_1}^{t_2} (C_2(t) - C_r) \cdot w_2(t) \cdot dt}{i \cdot w_{2_{medio}}^2} \tag{15}$$

The required flywheel inertia is therefore:

$$J_{flywheel} = J_{TOT} - J = 5.7671 \left[\mathrm{kg \cdot m^2}\right] \tag{16}$$

Considering stainless steel with density ρ = 7800 Kg/m^3, and thickness h = 100 mm several flywheel configurations were evaluated:

- Solid disk:

$$J_{flywheel} = \frac{1}{2} \cdot m_{solid} \cdot R_{solid}^2 = \frac{1}{2} \cdot \rho_{steel} \cdot \pi \cdot R_{solid}^4 \cdot h \tag{17}$$

with required radius R ≈ 0.26 [m] and mass m ≈ 168 kg.

- Hollow cylinder:

$$J_{flywheel} = \frac{1}{2} \cdot m_{hollow} \cdot \left(R_e^2 + R_i^2\right) = \frac{1}{2} \cdot \rho_{steel} \cdot \pi \cdot h \cdot \left(R_e^2 - R_i^2\right) \cdot \left(R_e^2 + R_i^2\right) \quad (18)$$

with inner-to-outer radius ratio $k = \frac{R_i}{R_e} = 0.75$. This yields slightly reduced mass for the same inertia.

Alternative designs included perforated and semi-solid structures, allowing trade-offs between mass, inertia, and manufacturability.

The effect of the flywheel is shown in Figure 7.

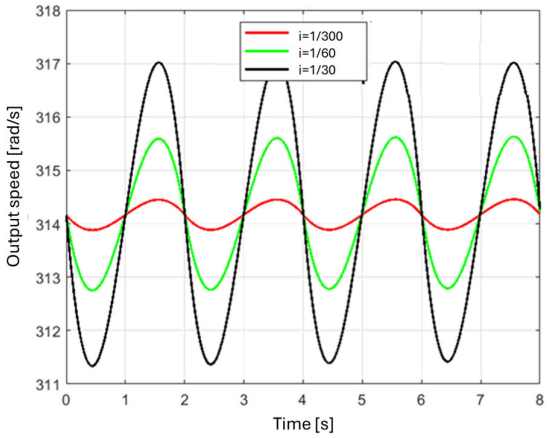

Figure 7. Effect of flywheel on output speed.

5. Efficiency Analysis

5.1. Efficiency of Mechanical System

The global efficiency of the mechanical system depends on transmission losses and flywheel stabilization [20,21]. The efficiency is defined as

$$\eta = \frac{P_{out}}{P_{in}} \quad (19)$$

where P_{out} is the mechanical power delivered to the alternator and P_{in} is the input wave-induced power.

For the studied configuration, the efficiency has been calculated considering the losses of all the components, as follows:

- **Recirculating Ball Guides**

  According to the THK catalog, the friction coefficient for an SHS guide is

$$\mu = 0.003$$

The efficiency is calculated as

$$\eta = 1/(1 + \mu)$$

Since the system consists of four carriages, the value is raised to the fourth power:

$$\eta = 0.988$$

- **Rack and Pinion Gears**

For the rack and pinion gear set, a high efficiency is assumed:

$$\eta = 0.99$$

- **Freewheels**

The system includes two NFR freewheels, each consisting of two 16,014 bearings (Figure 1).

From SKF data, the power loss for each bearing is obtained, and efficiency is expressed as

$$\eta = \frac{P_{transmitted} - P_{loss}}{P_{transmitted}} \quad (20)$$

This value is raised to the fourth power:

$$\eta = 0.999$$

Radial force is calculated assuming a pressure angle of $\alpha = 20^{\circ}$:

$$F_r = F_t \cdot tan\alpha = 1820\ \text{N} \quad (21)$$

Power loss at $\omega_1 = 83.33$ rpm: $P_{loss} = 0.22$ W.

- **UCP-208 Bearings**

A conservative assumption is made by assigning the full radial force to each bearing.
Power loss: P_loss = 1.9 W.
Efficiency:

$$\eta = \frac{P_{transmitted} - P_{loss}}{P_{transmitted}} = 0.999$$

- **Timing Belt**

For the toothed belt transmission, according to the SIT company catalogue, the efficiency is estimated as

$$\eta = 0.98$$

- **Epicyclic Gear Reducer**

From the manufacturer's catalog, the efficiency of the VRL 155 single-stage planetary reducer is

$$\eta = 0.95$$

- **UCP-207 Bearings**

For the two UCP-207 bearings, the radial force is estimated as

$$F_r = \left(F_t \cdot r_{motor\ pinion}\right) \cdot tan\alpha$$

At $\omega_2 = 3000$ rpm, the power loss is

$$P_{loss} = 51\ \text{W}$$

Efficiency:

$$\eta = \frac{P_{transmitted} - P_{loss}}{P_{transmitted}} = 0.972$$

- **Overall Efficiency**

https://doi.org/10.3390/engproc2026131043

The total mechanical efficiency is obtained by multiplying the efficiencies of all transmission elements:

$$\eta_{TOT} = 0.884$$

Thus, the resulting output mechanical power is

$$P_m = Pm_{MAX} \cdot \eta_m = 3471 \text{ W}$$

5.2. Efficiency of Hydraulic System

To evaluate potential advantages, the proposed mechanical solution was compared with a conventional hydraulic system of equivalent scale (Figure 8) [19]. Hydraulic PTOs, while widely used in oscillating body WECs, introduce several inefficiencies:

- Energy losses due to viscous friction in pumps, pipes, and hydraulic motors.
- Requirement of high-pressure circuits, accumulators, and control valves.
- Maintenance challenges due to fluid leakage and component wear in marine environments.

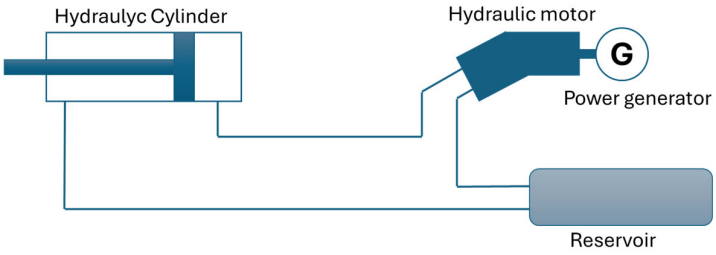

Figure 8. Schematic of hydraulic circuit.

The system consists of an array of articulated floaters anchored to a fixed structure. These floaters rise and fall following the wave motion, thereby driving a closed hydraulic circuit comprising the following elements:

- A hydraulic piston mechanically connected to the floater;
- A hydraulic accumulator that stores energy in the form of pressure;
- A hydraulic motor driven by the pressurized fluid;
- An electric generator coupled to the motor, which converts mechanical energy into electrical energy.

The vertical displacement of the floaters actuates the hydraulic piston, generating pressure in the fluid. This energy is temporarily stored in the accumulator and subsequently released in a controlled manner to drive the hydraulic motor, which in turn powers the generator.

To enable a direct comparison with our previously analyzed mechanical device, the following parameters are assumed to be equal for both systems:

- Output power from the hydraulic motor equal to that of our device: $P_{out} \approx 3.5$ kW;
- Piston stroke and oscillation period equal to those of the rack mechanism of our device.

The efficiency analysis is carried out by back-calculating losses, starting from the hydraulic motor and proceeding upstream in the system. According to manufacturer data (e.g., Bosch Rexroth A2FM and similar models), piston-type hydraulic motors—commonly employed in marine and offshore applications due to their robustness and efficiency—exhibit typical characteristics:

- Output power: 2–10 kW per unit;
- Operating pressure: 100–250 bar;
- Overall efficiency: 0.85–0.90.

For this study, an operating pressure is assumed as $p_{in,motor}$ = 210 bar with a motor efficiency of η_{motor} = 0.86, accounting for both mechanical and volumetric performance. The corresponding volumetric flow rate is then:

$$Q = \frac{P_{out}}{p_{in,motor} \cdot \eta_{motor}} \approx 11.5 \text{ L/min}$$

Assuming pressure losses in the circuit of $\Delta p_{circuit} = 5$ bar, the associated power dissipation is

$$\Delta P_{circuit} = Q \cdot \Delta p_{circuit} \approx 100 \text{ W}$$

The pressure at the accumulator outlet is therefore:

$$p_{out,accumulator} = p_{in,motor} + \Delta p_{circuit} = 215 \text{ bar}$$

Considering additional accumulator losses, $\Delta p_{accumulator} = 10$ bar, the accumulator inlet pressure becomes:

$$p_{in,accumulator} = p_{out,accumulator} + \Delta p_{accumulator} = 225 \text{ bar}$$

The accumulator efficiency is thus:

$$\eta_{accumulator} = \frac{p_{out,accumulator}}{p_{in,accumulator}} \approx 0.96$$

Proceeding to the piston stage, the outlet pressure is

$$p_{out,piston} = p_{in,accumulator} + \Delta p_{circuit} = 230 \text{ bar}$$

Assuming a piston efficiency of $\eta_{piston} = 0.95$, the required inlet pressure is

$$p_{in,piston} = \frac{p_{out,piston}}{\eta_{piston}} \approx 240 \text{ bar}$$

The overall input power to the system is then:

$$P_{in} = p_{in,piston} \cdot Q \approx 4.7 \text{ kW}$$

Accordingly, the total efficiency is

$$\eta_{TOT} = \frac{P_{out}}{P_{in}} = 0.746$$

5.3. Comparison of Efficiency Between Mechanical and Hydraulic Systems

The maximum force required by the floater on the piston is

$$F_{MAX} = \frac{P_{in}}{v_{MAX}} \approx 6000 \text{ N}$$

It follows that, to achieve the same output power as the mechanical system, the hydraulic system requires an additional 1000 N of force, since our direct mechanical device operated with only 5000 N. Furthermore, the hydraulic circuit results in power losses exceeding 1 kW, as only 3.5 kW are delivered at the motor from 4.7 kW at the piston input. In contrast, the mechanical device exhibited losses of less than 0.5 kW.

Finally, if the maximum available force due to wave conditions were limited to 5000 N (as initially assumed), both systems would receive an input power of approximately 4 kW.

https://doi.org/10.3390/engproc2026131043

However, the hydraulic device would only deliver about 3 kW of usable power to the generator, whereas the mechanical system maintained the target output of 3.5 kW.

6. Discussion

The analysis demonstrates that the proposed mechanical conversion system:

1. Effectively rectifies oscillatory motion, producing continuous unidirectional rotation through a dual-rack and freewheel arrangement.
2. Amplifies angular velocity via belt and planetary transmission, reaching rotational speeds compatible with alternator operation (up to ~3000 rpm).
3. Stabilizes operation with a flywheel, ensuring a degree of irregularity within acceptable limits for electrical generation.
4. Delivers competitive efficiency, outperforming conventional hydraulic systems in theoretical terms, though subject to mechanical durability constraints.

The analysis of the flywheel confirms that angular acceleration and velocity oscillations are substantially reduced after coupling with the flywheel, leading to smoother power output.

Overall, the mechanical PTO with integrated flywheel emerges as a promising alternative for wave energy conversion, especially in applications where simplicity, robustness, and efficiency are prioritized over modular scalability.

7. Conclusions

This work has presented a detailed study of a novel mechanical system for wave energy conversion, emphasizing its kinematic and dynamic behavior, flywheel design, and efficiency. After reviewing the state of the art of Wave Energy Converters (WECs), the analysis focused on a rack-and-pinion mechanism equipped with freewheels to transform bidirectional linear motion into unidirectional rotation.

The results demonstrated that:

- The device can effectively rectify oscillatory motion, ensuring continuous rotary output.
- The inclusion of a transmission system and planetary gear raises the rotational speed to levels compatible with commercial alternators.
- The flywheel is essential for stabilizing rotational irregularities, reducing the degree of irregularity below the threshold required for efficient electrical generation.
- The system achieves a maximum mechanical power output of approximately 3.9 kW, with efficiency estimated at 70–80%.
- Compared to hydraulic PTO systems, the mechanical configuration offers higher theoretical efficiency, reduced complexity, and simpler maintenance, though it requires robust design to withstand marine conditions.

From a broader perspective, this study highlights that while wave energy conversion technologies are still developing, mechanical PTO systems with integrated flywheels provide a promising path toward cost-effective and reliable exploitation of ocean energy. Future research should focus on experimental validation, material optimization for marine durability, and integration of control systems to enhance adaptability under variable wave conditions.

Author Contributions: Conceptualization, A.M.; methodology, A.M.; validation, L.M. (Luigi Mazza), L.M. (Luca Margaria) and G.C.; formal analysis, A.M. and L.M. (Luca Margaria); investigation, A.M., L.M. (Luigi Mazza), L.M. (Luca Margaria) and G.C.; resources, A.M.; writing—original draft preparation, all authors.; writing—review and editing, A.M., L.M. (Luigi Mazza), L.M. (Luca Margaria) and G.C.; project administration, A.M.; funding acquisition, A.M. All authors have read and agreed to the published version of the manuscript.

Funding: This publication is part of the project NODES, which has received funding from the MUR—M4C2 1.5 of PNRR funded by the European Union-Next Generation EU (grant agreement no. ECS00000036).

Institutional Review Board Statement: Not applicable.

Informed Consent Statement: Not applicable.

Data Availability Statement: The original contributions presented in this study are included in the article. Further inquiries can be directed to the corresponding author.

Acknowledgments: The authors acknowledge Makita Italia s.p.a. for the technical support.

Conflicts of Interest: The authors declare no conflict of interest.

References

1. Benassai, G.; Dattero, M.; Maffucci, A. Wave Energy Conversion Systems: Optimal Localization Procedure. *WIT Trans. Ecol. Environ.* **2009**, *126*, 129–138. [CrossRef]
2. Falcão, A.F.D.O. Wave Energy Utilization: A Review of the Technologies. *Renew. Sustain. Energy Rev.* **2010**, *14*, 899–918. [CrossRef]
3. Zhang, Y.; Zhao, Y.; Sun, W.; Li, J. Ocean Wave Energy Converters: Technical Principle, Device Realization, and Performance Evaluation. *Renew. Sustain. Energy Rev.* **2021**, *141*, 110764. [CrossRef]
4. Bruno, M.; Maccanti, M.; Pulselli, R.M.; Sabbetta, A.; Neri, E.; Patrizi, N.; Bastianoni, S. Benchmarking marine renewable energy technologies through LCA: Wave energy converters in the Mediterranean. *Front. Energy Res.* **2022**, *10*, 980557. [CrossRef]
5. Mura, A. Sistema per una Produzione di Energia Elettrica o Meccanica dal Moto Ondoso. Italian Patent ITBS20090157A1, 14 September 2012.
6. Novo, R. A Preliminay Study about Methods for Harvesting Energy from Marine Resources. Bachelor's Thesis, Politecnico di Torino, Turin, Italy, 2015. [CrossRef]
7. Lian, J.; Wang, X.; Wang, X.; Wu, D. Research on Wave Energy Converters. *Energies* **2024**, *17*, 1577. [CrossRef]
8. Gobato, R.; Gobato, A.; Fedrigo, D.F.G. Study Pelamis System to Capture Energy of Ocean Wave. *arXiv* **2015**. [CrossRef]
9. Penalba, M.; Ringwood, J.V. A Review of Wave-to-Wire Models for Wave Energy Converters. *Energies* **2016**, *9*, 506. [CrossRef]
10. Carraro, M. Wave Energy Extraction Using Vertical Motion Buoys: Modeling and Control (Estrazione di Energia Dalle Onde Tramite boe a Moto Verticale: Modellizzazione e Controllo). Master Thesis, Università degli Studi di Padova, Padova, Italy, 2009–2010. (In Italian)
11. Eriksson, M.; Isberg, J.; Leijon, M. Hydrodynamic Modelling of a Direct Drive Wave Energy Converter. *Int. J. Eng. Sci.* **2005**, *43*, 1377–1387. [CrossRef]
12. Heath, T.V. Chapter 334—The Development and Installation of the Limpet Wave Energy Converter. In *World Renewable Energy Congress VI*; Pergamon: Bergama, Turkey, 2000; pp. 1619–1622. [CrossRef]
13. OE-Buoy. Available online: https://oceanenergy.ie/oe-buoy/ (accessed on 5 July 2025).
14. Wave Dragon Project Documentation. Available online: https://tethys-engineering.pnnl.gov/sites/default/files/publications/Wave-Dragon-2009.pdf (accessed on 5 July 2025).
15. Contestabile, P.; Crispino, G.; Di Lauro, E.; Ferrante, V.; Gisonni, C.; Vicinanza, D. Overtopping breakwater for wave Energy Conversion: Review of state of art, recent advancements and what lies ahead. *Renew. Energy* **2020**, *147*, 705–718. [CrossRef]
16. Archimedes Waveswing. Available online: https://awsocean.com/archimedes-waveswing/ (accessed on 5 July 2025).
17. ISWEC Project. Available online: https://morenergylab.polito.it/iswec/ (accessed on 5 July 2025).
18. Carcas, M. The_Pelamis_Wave_Energu_Converter. Available online: https://energiatalgud.ee/sites/default/files/images_sala/3/3a/Carcas%2C_M._The_Pelamis_Wave_Energu_Converter.pdf (accessed on 5 July 2025).
19. Eco Wave Power. Company Reports. Available online: https://www.ecowavepower.com/ (accessed on 5 July 2025).
20. Ferraresi, G.; Raparelli, T. *Meccanica Applicata*, 3rd ed.; CLUT Editrice: Torino, Italy, 2007.
21. Fasana, A.; Marchesiello, S. *Meccanica delle Vibrazioni*; CLUT Editrice: Torino, Italy, 2006.

Disclaimer/Publisher's Note: The statements, opinions and data contained in all publications are solely those of the individual author(s) and contributor(s) and not of MDPI and/or the editor(s). MDPI and/or the editor(s) disclaim responsibility for any injury to people or property resulting from any ideas, methods, instructions or products referred to in the content.